

# MULTIPACTING IN CROSSED RF FIELDS NEAR CAVITY EQUATOR

Valery Shemelin\*

Laboratory for Elementary-Particle Physics, Cornell University, Ithaca, NY 14853

## Abstract

Electric and magnetic fields near the cavity equator are presented in the form of Taylor series. Comparisons with numerical calculations made with the SLANS code for the TESLA cavity cells, as well as with the analytical solution for a spherical cavity are done. These fields are used for solving the equations of motion. It appears that for description of motion, only the main terms of the expansion are essential, but the value of coefficients for the electric field components depend on details of magnetic field behavior on the boundary. Equations of motion are solved for electrons moving in crossed RF fields near the cavity equator. Based on the analysis of these equations, general features of multipacting in this area are obtained. The “experimental” formulas for multipacting zones are explained and their dependence on the cavity geometries is shown. Developed approach allows evaluation of multipacting in a cavity without simulations but after an analysis of fields in the equatorial region. These fields can be computed by any code used for cavity calculation.

## INTRODUCTION

Results of multipacting simulations suggest a possible way of better understanding of the phenomenon. Let us consider the trajectory obtained for a cavity [1], Fig. 1. The calculations were performed with MultiPac [2]. One can see that the dimensions of the trajectory are very small in comparison with the cavity dimensions. It is clear that the magnetic field has as big influence on the motion as the electric field. At the same time the amplitude of the magnetic field is nearly constant within so small change of coordinates near the equator. These features can be used in derivation of the equations of motion.

Of course, integration of equations of motion is performed in any simulation. But these are most general equations taking into account fields in the whole cavity. We see our task in using simplified presentation of fields in the region of interest. The analytical presentation of the equations can give figures of merit that determine the phenomenon. For example, for multipacting in a flat gap, the value of  $fd$ , the frequency times the gap length, defines limits of normalized voltage  $\xi = eU/m\omega^2 d^2$  across the gap where the discharge takes place. It appears that in the case of multipacting near the cavity equator, the determining value is  $M = eB_0/m\omega$ . Here  $e/m$  is the specific charge of electron,  $U$  is the voltage across the gap,  $B_0$  is the magnetic field at the equator, and  $\omega = 2\pi f$  is the angular frequency of oscillations.

\* vs65@cornell.edu

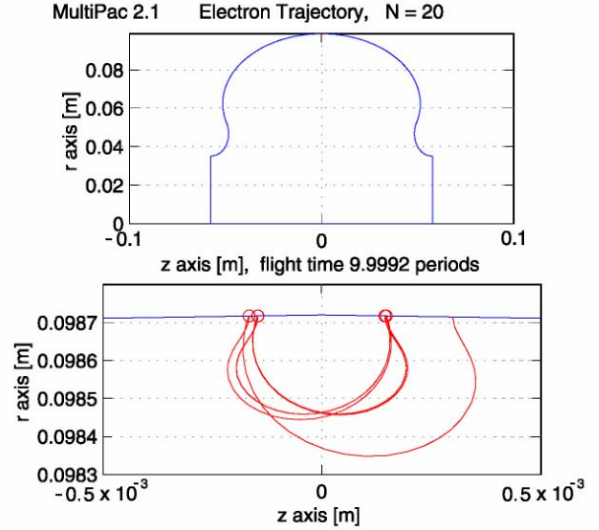


Fig. 1: Resonant electron orbit at a peak surface field level about 37 MV/m [1].

## FIELDS NEAR EQUATOR

We describe fields near the cavity equator in the cylindrical system of coordinates,  $\rho$ ,  $\varphi$ ,  $\zeta$ , Fig. 2. Let us present the fields in a form of series up to the second ( $E_\zeta, E_\rho$ ) and the third ( $B_\varphi$ ) order of increments:

$$\begin{aligned} E_\zeta &= \alpha_0 (R_{eq} - \rho) + \alpha_1 (R_{eq} - \rho)^2 + \alpha_3 \zeta^2, \\ E_\rho &= \beta_0 \zeta + \beta_4 (R_{eq} - \rho) \zeta, \\ B_\varphi &= B_0 [1 + a(R_{eq} - \rho) + g(R_{eq} - \rho)^2 + h\zeta^2 + \\ &\quad + q(R_{eq} - \rho)^3 + s(R_{eq} - \rho)\zeta^2]. \end{aligned} \quad (1)$$

Not all the powers of expansion are presented because  $E_\zeta$  and  $B_\varphi$  are even and  $E_\rho$  is an odd function of  $\zeta$ .

For calculation of coefficients  $a, g, h, \dots, \alpha_0, \dots, \beta_0, \dots$  we used Maxwell equations in the form

$$\text{rot} \vec{E} = -\partial \vec{B} / \partial t, \quad \text{rot} \vec{H} = \partial \vec{D} / \partial t, \quad \text{div} \vec{E} = 0, \quad (2)$$

with  $\vec{B} = \mu_0 \vec{H}$  and  $\vec{D} = \epsilon_0 \vec{E}$ . We equated coefficients standing before equal terms of the expansion.

The condition that the vector  $\vec{E}$  is normal to the surface gives

$$2\beta_0 = \alpha_0 + 2R_c \alpha_3. \quad (3)$$

For the value of  $B_\varphi$ , we can compare our results with the fields in a spherical cavity if we take into account the quadratic term *along the border line*:

$$B_\varphi = B_0 (1 - \nu \zeta^2 / 2R_c^2).$$

For a spherical cavity  $\nu = 1$  ( $B_\varphi \propto \sin \theta$ ,  $\theta \approx \pi/2$ ).

This equation together with  $B_\varphi$  from (1) gives:

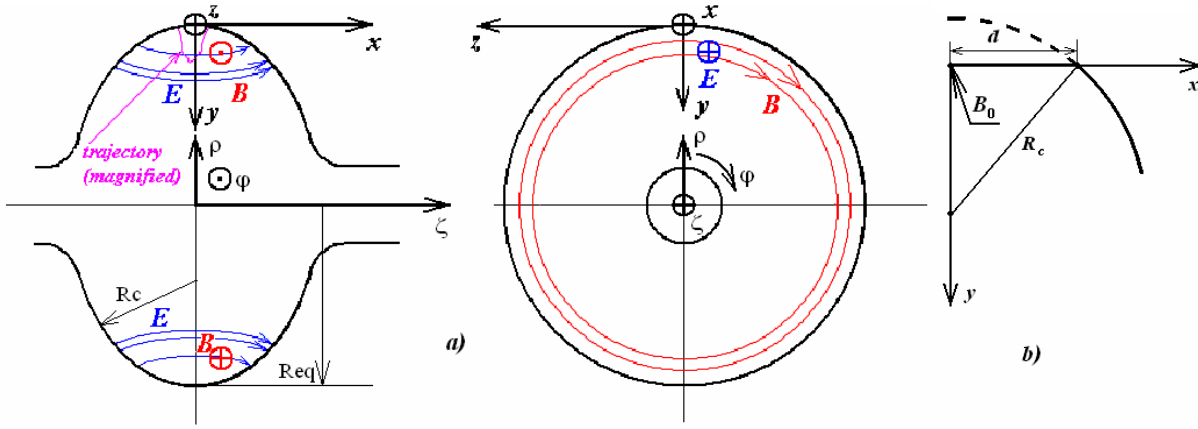


Fig. 2: Coordinate systems for calculations (a) and alternative geometry with a partly flat profile line (b).

$$a + 2R_c h + v/R_c = 0. \quad (4)$$

Now one can obtain the chain of solutions for the coefficients:

$$\begin{aligned} a &= 1/R_{eq}, & h &= -a/2R_c - v/2R_c^2, \\ \beta_0 &= -2B_0 c^2 h/\omega, & \alpha_0 &= \omega B_0 - \beta_0, \\ \alpha_3 &= (2\beta_0 - \alpha_0)/2R_c, & \beta_4 &= \beta_0/R_{eq} + 2\alpha_3, \\ s &= -\omega\beta_4/2B_0 c^2, & g &= 1/R_{eq}^2 - \omega\alpha_0/2B_0 c^2, \\ \alpha_1 &= (\omega B_0 a - \beta_4)/2, & q &= g/3R_{eq} + 2/3R_{eq}^3 - \omega\alpha_1/3B_0 c^2. \end{aligned} \quad (5)$$

Here  $c = 1/\sqrt{\mu_0 \epsilon_0}$  is the speed of light.

If a cavity has a short flat region near the equator, Fig. 2b, formulae for  $h$  and  $\alpha_3$  in (5) should be changed by

$$h = -v/2R_c^2 \text{ and } \alpha_3 = 0 \quad (5a)$$

if the trajectory is confined in a region  $x \ll d$ ,  $y \ll d$ . The values of  $\alpha_0$  and  $\beta_0$  that will be needed further can be also taken directly from the field calculations.

To check validity of the proposed approach two cavities were analyzed: fields for the TESLA regular cell are calculated using SLANS [3], fields for the fundamental mode of the spherical 1.3 GHz cavity are found analytically. Then both solutions are found using the proposed expansion in the area with  $|z| \leq 5$  mm and  $y \leq 2$  mm.

The differences between the solutions for the TESLA cell are:  $< 3$  % for  $E_r$ ,  $< 1$  % for  $E_z$ , and  $< 0.01$  % for  $B_\phi$ .

The differences for the spherical cavity are:  $< 0.3$  % for  $E_r$ ,  $< 0.1$  % for  $E_z$ , and  $< 0.0003$  % for  $B_\phi$ .

## EQUATIONS OF MOTION

The system of coordinates, fields in the equatorial area and a possible trajectory of an electron in the cavity are shown in Fig. 2.

Let us present the magnetic and electric field in this region in the form

$$\begin{aligned} B_z &= -B_0 \cos \theta, \\ E_x &= \alpha \cdot y \cdot \sin \theta, \\ E_y &= -\beta \cdot x \cdot \sin \theta. \end{aligned} \quad (6)$$

Here  $\theta = \omega t$ ,  $t$  is time,  $\alpha$  and  $\beta$  are coefficients of proportionality. We will use  $\alpha = \alpha_0$  and  $\beta = \beta_0$  from (5). Adding of higher terms of the expansions has an insignificant effect on the results. However, for calculation of  $\alpha_0$  and  $\beta_0$  the coefficient  $h$  describing dependence of the magnetic field on  $\zeta^2$  should be used, see (5) and (5a).

Now we can write the equations of motion taking into account these three components of fields:

$$\begin{aligned} e(E_x + \dot{y}B_z) &= m\ddot{x}, \\ e(E_y - \dot{x}B_z) &= m\ddot{y}. \end{aligned} \quad (7)$$

The charge of electron is taken positive to simplify writing. Dots designate derivatives with respect to time.

Replacing derivatives with respect to time by derivatives with respect to the phase angle  $\theta$  (designated by primes), so that

$$\dot{x} = \omega x', \quad \ddot{x} = \omega^2 x'', \text{ and so on,}$$

one can obtain the equations of motion in a normalized form:

$$\begin{aligned} x'' &= M[(1-p)y \sin \theta - y' \cos \theta], \\ y'' &= M(-px \sin \theta + x' \cos \theta). \end{aligned} \quad (8)$$

Here  $M = eB_0/m\omega$  is the magnetic parameter of the motion and  $p = \beta/(\alpha + \beta) = \beta/\omega B_0$  can be named the transverse parameter because it is proportional to the electric field component normal to the surface, *i.e.* transverse in relation to the main electric field on the axis. From (5), one can obtain

$$p = (c^2/\omega^2) \cdot (a/R_c + v/R_c^2) \quad (9)$$

or, in the case (5a),

$$p = c^2 v / \omega^2 R_c^2. \quad (9a)$$

The set (8) can be rewritten as a set of first order equations that is convenient for solving, *e.g.*, as a MathCAD task:

$$\begin{aligned} x'_0 &= x_1, \\ x'_1 &= M[(1-p)x_2 \sin \theta - x_3 \cos \theta], \\ x'_2 &= x_3, \\ x'_3 &= M(-px_0 \sin \theta + x_1 \cos \theta). \end{aligned} \quad (10)$$

## CONDITION OF STABILITY

In the case when multipacting occurs near the cavity equator, the starting electron should be described both by the phase of the field and the distance from the equator because the electric field  $E_y$  changes with this distance  $x$ , see (6). If the electron has not an equilibrium initial phase and position, after the flight to the next impinge onto the surface, its phase and position will change:

$$\begin{aligned}\Delta\theta_2 &= (\partial\theta_2/\partial\theta_1)\Delta\theta_1 + (\partial\theta_2/\partial x_1)\Delta x_1, \\ \Delta x_2 &= (\partial x_2/\partial\theta_1)\Delta\theta_1 + (\partial x_2/\partial x_1)\Delta x_1,\end{aligned}\quad (11)$$

where  $\Delta\theta_1$  and  $\Delta x_1$  are deviations from the equilibrium phase and position, respectively, at the start point,  $\Delta\theta_2$  and  $\Delta x_2$  are deviations after the flight. The derivatives in (11) are taken for the equilibrium situation when the time of flight is equal to the integer odd number of half-periods:

$$\theta_2 - \theta_1 = (2n - 1)\pi.$$

The system (11) can be written as a matrix product:

$$\begin{pmatrix} \Delta\theta_2 \\ \Delta x_2 \end{pmatrix} = \begin{pmatrix} a & b \\ c & d \end{pmatrix} \begin{pmatrix} \Delta\theta_1 \\ \Delta x_1 \end{pmatrix} \equiv A \begin{pmatrix} \Delta\theta_1 \\ \Delta x_1 \end{pmatrix}.$$

After the  $N$ th flight, the deviations are

$$\begin{pmatrix} \Delta\theta_{N+1} \\ \Delta x_{N+1} \end{pmatrix} = A^N \begin{pmatrix} \Delta\theta_1 \\ \Delta x_1 \end{pmatrix}.$$

So, for stability, it is necessary that

$$\lim_{N \rightarrow \infty} A^N = 0,$$

and this requirement is fulfilled if the characteristic roots of the matrix equation

$$A - \lambda I = 0, \quad (12)$$

where  $I$  is a unitary matrix, meet the conditions

$$|\lambda_1| < 1, \quad |\lambda_2| < 1. \quad (13)$$

Derivatives for (11) were found numerically solving the equations of motion (10) for different  $p$  and  $M$ , and substituted into equation (12). The area where the conditions (13) are met is the multipacting area. It is shown in Fig. 3 as the boundary of stability.

## COMPARISON WITH EXPERIMENT

Maximal energy of primary electrons for each value of  $p$  is reached on the line shown in Fig. 3. Lines of equal energy of primary electrons  $E_p$  for the most important region of  $p$  between 0.2 and 0.4 are also shown. Energy of secondary electrons  $E_s$  is taken to be 2 eV. Because of linearity of equations (8) the impact energy  $E_p$  is proportional to  $E_s$ . So, if one takes  $E_s = 4$  eV, all numbers for  $E_p$  should be doubled. It is seen that  $E_p$  is rather small for multipacting in the cavity 1 (see subscription to the figure) and the cavity 4 is most vulnerable to multipacting. To decrease  $E_p$ , the lower value of  $p$  is needed. This can be done choosing the

geometry. For example, a small flatness ( $d \ll R_c$ , Fig. 2b) should help, see (9) and (9a).

The formula for the magnetic parameter  $M = eB_0/m\omega$  can be rewritten in a form

$$B_0 [\text{mT}] = 35.7 M \cdot f [\text{GHz}],$$

where limits of  $M$  depend on the value of  $p$ . Cavities with the same frequency can have different regions of multipacting having different geometry. This formula is similar to experimental formulae [4, 5, 6] but now it gives a clear physical explanation.

Because of space limitations only the most important case of two-point multipacting of the first order ( $n = 1$ ) in the crossed fields of equatorial area is shortly described. Other details will be presented somewhere.

The author wishes to express a great gratitude to Sergey Belomestnykh for numerous discussions and careful reading of the manuscript. I also thank Rongli Geng for useful remarks.

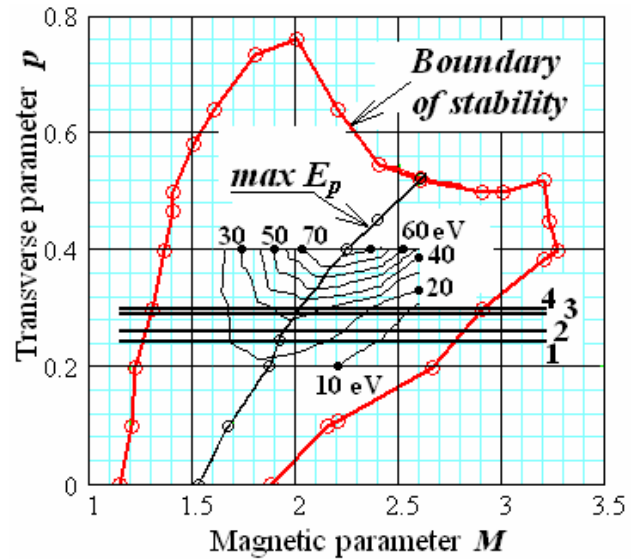


Fig. 3: Equatorial cross-field multipacting zone with  $n = 1$ . Examples for several geometries: 1 – Cornell 200 MHz cavity, 2 – TESLA optimized [1], and 3 – TESLA original cavity, 4 – TRISTAN 500 MHz cavity [6].

## REFERENCES

- [1] V. Shemelin, H. Padamsee, R.L. Geng. Nucl. Instr. Methods Phys. Res.-A, **496**, 2003.
- [2] P. Ylä-Oijala, J. Lakkariinen, S. Järvenpää, M. Ukkola, Multipac 2.1, Rolf Nevanlinna Institute, Helsinki, 2001.
- [3] D. Myakishev, V. Yakovlev. Particle Acc. Conf. and Int. Conf. on High Energy Acc. May 1 – 5, 1995, Texas.
- [4] R. Geng. Proc. 2003 Particle Acc. Conf. May 12-16, 2003, Portland, Oregon.
- [5] P. Fabbricatore, G. Gemme, R. Musenich, R. Parodi, S. Pittaluga. Proc. of the 7<sup>th</sup> SRF Workshop, October 17-20, 1995, Gif sur Yvette, France.
- [6] K. Saito. The 10<sup>th</sup> Workshop on RF Superconductivity, 2001, Tsukuba, Japan.